JOURNAL OF SOLID STATE CHEMISTRY 104, 59–73 (1993)

A Reinvestigation of Low-Carnegieite by XRD, NMR, and TEM

JOHN G. THOMPSON* AND RAY L. WITHERS

Research School of Chemistry, Australian National University, Canberra, Australian Capital Territory 0200, Australia

ANDREW K. WHITTAKER

Centre for Magnetic Resonance, University of Queensland, Queensland 4072, Australia

RICHARD M. TRAILL

Department of Chemistry, Monash University, Clayton, Victoria 3168, Australia

AND JOHN D. FITZ GERALD

Research School of Earth Sciences, Australian National University, Canberra, Australian Capital Territory 0200, Australia

Received October 29, 1992; accepted November 9, 1992

The crystal structure of low-carnegieite, $NaAlSiO_4$, has been reinvestigated by a combination of X-ray powder diffraction, transmission electron microscopy, solid-state ^{29}Si and ^{27}Al MAS NMR spectroscopy, and electron microprobe analysis. With sufficient homogenization of component oxides and annealing at 1673 K it was possible to obtain a single crystalline phase which could be indexed to an orthorhombic unit cell: $Pb2_1a$, $a = 10.261(1)$, $b = 14.030(2)$, $c = 5.1566(6)$ Å. Electron microprobe analysis confirmed the stoichiometry to be $NaAlSiO_4$. ^{29}Si and ^{27}Al NMR spectroscopy verified the perfect Si : Al ordering. It is now clear from the present work that previous attempts to synthesize low-carnegieite all suffered from incomplete reaction and the presence of other phases. One of these phases has been identified as having a large hexagonal unit cell with $a = 13.97(2)$, $c = 15.03(2)$ Å.

Introduction

The crystal structure of carnegieite, $NaAlSiO_4$, is closely related to that of cristobalite, the high-temperature polymorph of SiO_2. It can be described as a "stuffed" derivative of cristobalite (*1*, *2*) in which half of the cavities in the SiO_2 framework are filled with sodium atoms (Fig. 1). It exists as the stable polymorph of $NaAlSiO_4$ between 1523 K and its melting point at 1799 ± 2 K (*3*). Below 1520 K the stable polymorph of $NaAlSiO_4$ has the nepheline structure,

* Author to whom correspondence should be addressed.

0022-4596/93 $5.00

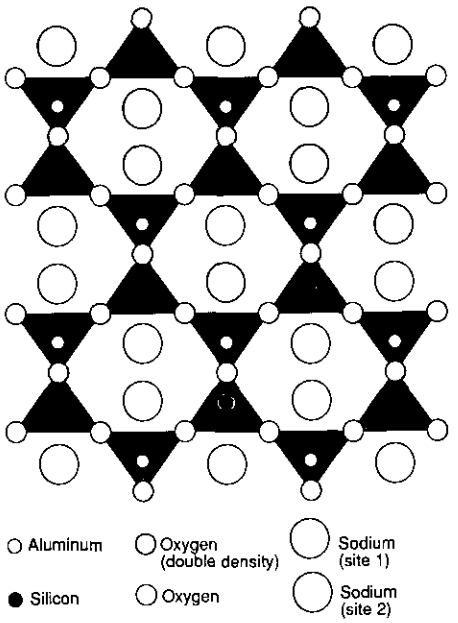

FIG. 1. Polyhedral representation of idealized high-carnegieite projected along the cubic [110] direction. In this direction the SiO_4 and AlO_4 tetrahedra project, as do the two symmetry inequivalent idealized Na sites.

which is a "stuffed" derivative of another polymorph of silica, namely tridymite (*4*).

The early work on high-carnegieite (*5*, *6*) determined that it had a simple cubic structure with space group symmetry $P2_13$ or $F\bar{4}3m$ with cubic unit cell dimension a = 7.37(2) Å. It was also shown that, upon cooling relatively quickly (e.g., 1 min) to room temperature, high-carnegieite underwent a non-reconstructive phase transition at 940 ± 5 K (*7*) to adopt a lower symmetry crystal structure. The exact crystal structure of low-carnegieite has been difficult to determine owing to the inability to grow single crystals.

There have been several reports of X-ray powder diffraction (XRD) data for low-carnegieite (*7–9*). Klingenberg and Felsche (*7*) observed that there was poor agreement between the Guinier data (103 observed reflections) for their specimen and the XRD data reported by previous workers. They recorded electron diffraction photographs in a transmission electron microscope to assist in indexing their XRD data and attributed the above differences principally to differing thermal history of samples.

Klingenberg and Felsche (*7*) successfully indexed their 103 reflections to a triclinic unit cell, $P1$ or $P\bar{1}$, a = 5.0347 (6), b = 5.0822(7), c = 16.910(2), α = 99.00(1), β = 81.50(1), γ = 119.09(1)°. They described the unit cell as a superstructure of cristobalite type. The problem with this assignment was the intensity of some of the so-called superstructure reflections. For example, the ninth reflection observed (indexed as $10\bar{4}$ in the triclinic unit cell and by their definition a superstructure reflection) had a relative intensity (I/I_0) of 51%. Given that low-carnegieite is necessarily closely related to high-carnegieite it would be expected that the "superstructure" reflections would be relatively weak compared to the parent $F\bar{4}3m$ reflections. This is certainly true for low-cristobalite when compared with the parent $Fd3m$ reflections.

Another concern was the size and the low symmetry of the triclinic unit cell and the lack of low angle data (the largest **d**-spacing was 4.394 Å). To illustrate the problem of uniquely determining the unit cell under such circumstances, for the Klingenberg and Felsche unit cell there are 699 calculated reflections out to a d-spacing of 1.038 Å, of which 103 were observed. With such a density of calculated reflections, particularly at higher angle, it is unlikely that a reflection could not be indexed to the reported unit cell.

Borchert and Keidel (*10*) were able to prepare Na_2O-rich carnegieites with the formula $Na_4Al_4Si_4O_{16} \cdot nNa_2O$, n = 1–2, by reaction of kaolinite with NaOH and subsequent heating. The excess Na_2O stabilized the high-temperature structure giving a cubic unit cell with space group symmetry $F\bar{4}3m$. Subsequent work (*11*) confirmed that the

carnegieite structure could accommodate a substantial amount of Na_2O in the remaining cavities in the aluminosilicate framework. In contrast with the earlier work (*10*) they achieved concentrations of 0.01–0.33 Na_2O intercalated into the carnegieite "host lattice." These observations of a significant "carnegieite" solid solution in the pseudoternary $NaO_{0.5}$–$AlO_{1.5}$–SiO_2 system suggested to us that the system may be more complicated than first believed.

As a result of our concerns about the interpretation of XRD data by previous workers we decided to attempt to reproduce their work, with particular emphasis on verifying the consistency of the X-ray powder diffraction data with electron diffraction data from the same specimen.

Experimental

Synthesis

All specimens were from AR grade Na_2CO_3, $Al(OH)_3$, and SiO_2. A 1 : 2 : 2 mole ratio mixture of the components was thoroughly ground in a mortar and pestle under acetone. Initial attempts to reproduce the XRD results of Klingenberg and Felsche (*7*) by following their experimental conditions were unsuccessful; i.e., "heating the composition for 24 h at 1073 K, subsequent annealing at 1573 K for another 24 h, and immersing the crucible in a water bath." XRD analysis following subsequent cycles of grinding and heating suggested two possibilities. Either the composition $NaAlSiO_4$ occurred in a 2- or 3-phase region of the $NaO_{0.5}$–$AlO_{1.5}$–SiO_2 phase diagram, or the specimen was still far from thermodynamic equilibrium prior to quenching.

To test the former possibility specimens were prepared at four compositions away from the 1 : 1 : 1 stoichiometry of $NaAlSiO_4$: i.e., $Na_{0.95}Al_{0.95}Si_{1.05}O_4$, $Na_{1.05}Al_{1.05}Si_{0.95}O_4$, $Na_{0.95}Al_{1.05}Si_{1.00}O_{4.05}$, $Na_{1.05}Al_{0.95}Si_{1.00}O_{3.95}$. The XRD data for these four specimens were virtually identical suggesting that the latter possibility, namely sluggish kinetics, was the problem.

In order to accelerate the reaction the 1 : 1 : 1 specimen, after its initial pretreatment for 24 h at 1073 K, was heated to 1873 K for 1 h, then annealed at 1673 K for 40 h. The 1873 K and 1673 K heating was repeated after an intermediate grinding and pelleting. The resultant material, as discussed below, gave a reproducible XRD pattern free of the problems discussed above.

Characterization

Specimens were examined by various complementary analytical techniques to follow the course of reaction and to characterize the reaction products.

(i) X-ray powder diffraction (XRD). All specimens were examined by XRD using a Guinier–Hägg camera with monochromated Cu$K\alpha_1$ radiation. For accurate measurement of diffraction lines for the purposes of refining the unit cell dimensions, Si (NBS No. 640) was used as an internal standard.

(ii) Transmission electron microscopy (TEM)/electron diffraction. Finely ground specimen was dispersed onto a holey carbon grid. Electron diffraction patterns were recorded using JEOL 100CX and Philips EM430 microscopes, the latter equipped with a Si detector for energy dispersive spectroscopy (EDS) supported by a PV9900 analysis system.

(iii) NMR results were obtained on a Bruker MSL300 spectrometer operating at 59.627 and 78.205 MHz for ^{29}Si and ^{27}Al, respectively. Samples were spun at the magic angle at 5 kHz (^{29}Si) or at 10 kHz (^{27}Al) in Bruker double air bearing probes. ^{29}Si spectra were collected using the single pulse excitation technique with a 60 sec recycle. ^{27}Al spectra were obtained using the single pulse excitation technique with an rf pulse time of 1 sec. A pulse recycle delay of 1 sec was used for these experiments.

(iv) Determination of chemical compositions was carried out in a Cameca Camebax electron microprobe using EDS with the mineral anorthoclase as an analytical standard.

Results

XRD

As mentioned above, the initial attempts to synthesize single phase low-carnegieite following the procedure described by Klingenberg and Felsche (*7*) led to a frustrating lack of reproducibility of lines in the XRD patterns. From the initial syntheses at 1573 K the only clearly reproducible lines, in terms of position and relative intensities, from the various syntheses belonged to a subset of seven strong lines. These could be indexed to a large hexagonal unit cell with dimensions $a = 13.97(2)$, $c = 15.03(2)$ Å. These lines were also present in the data of Klingenberg and Felsche (*7*). In some of the syntheses, particularly the Al_2O_3-rich compositions, there were also a number of low-angle lines which belonged to β- or β''-aluminas. The silica-rich specimen was largely amorphous.

The XRD pattern for the 1 : 1 : 1 specimen, which had been thoroughly homogenized and annealed once at 1673 K, was strikingly different from all the previous patterns, but there were still weak lines due to the hexagonal phase and the rest of the lines were not completely sharp. Further homogenization and annealing at 1673 K gave a clean XRD pattern which could be indexed completely by the following orthorhombic unit cell: $a = 10.261(1)$, $b = 14.030(2)$, $c = 5.1566(6)$ Å. These data are presented in Table I. Closer inspection of these data reveals symmetry conditions, such that the Bravais lattice is P, and both $0kl$, $k = 2n$ and $hk0$, $h = 2n$ hold. These conditions limit the space group of low-carnegieite to Pb_a.

Figure 2 shows densitometer traces of the Guinier–Hägg films for both low-carnegieite and a 1 : 1 : 1 multiphase specimen prepared under the conditions described by Klingenberg and Felsche (*7*). The lower-angle lines ($\leq 48°$ 2θ) identified as belonging to the hexagonal phase are indicated for the multiphase specimen.

The XRD data ($\leq 48°$ 2θ) for the 1 : 1 : 1 multiphase specimen described above and shown in Fig. 1 are presented in Table II together with the equivalent data listed in Tables 1 and 2 of Klingenberg and Felsche (*7*). While these two data sets are not identical there is remarkable similarity, particularly for the strong lines belonging to the hexagonal phase. The hexagonal lines have been assigned according to the refined unit cell given above.

TEM/Electron Diffraction

Initial investigation by TEM showed that low-carnegieite specimens were somewhat sensitive to the electron beam and, hence, care had to be taken to successfully record the appropriate diffraction patterns. Provided such care was taken, however, the results were completely reproducible. Figure 3 shows (a) a [100] zone axis Convergent Beam Pattern (CBP), (b) a corresponding Selected Area Diffraction Pattern (SADP) but tilted a few degrees off [100], (c) an [010] zone axis SADP, and (d) an [001] zone axis SADP of the single crystalline phase low-carnegieite.

All of the zone axes presented in Fig. 3 display a subset of strong Bragg reflections corresponding to the underlying $F\bar{4}3m$ high-carnegieite-type average or parent structure. The real and reciprocal space unit cell relationships between the parent cubic structure and the low-carnegieite structure are illustrated in Fig. 4. In terms of the strong Bragg reflections corresponding to the underlying $F\bar{4}3m$, high-carnegieite-type, average structure the new reciprocal lattice basis vectors can be expressed as $\mathbf{a}^* = \frac{1}{4}(2,0,2)^*$, $\mathbf{b}^* =$

TABLE I

POWDER DIFFRACTION DATA FOR LOW-CARNEGIEITE, $NaAlSiO_4$

No.	*hkl*	d_{calc}	d_{obs}	I/I_0	No.	*hkl*	d_{calc}	d_{obs}	I/I_0
1	111	4.377	4.371	4	37	361	1.808	1.807	4
2	021	4.155	4.155	100	38	252	1.780	1.780	8
3	220	4.141	4.136	100	39	080	1.754	1.754	19
4	121	3.851	3.849	4	40	162	1.708	1.708	3
5	201	3.637	3.637	12	41	103	1.695	1.695	4
6	040	3.507	3.507	8	42	541	1.675	1.675	2
7	230	3.456	3.457	28	43	023	1.669	1.669	11
8	131	3.282	3.282	20	44	620	1.662	1.661	12
9	231	2.871	2.871	31	45	262	1.641	*	2
10	141	2.791	2.792	26	46	442	1.614	1.614	4
11	321	2.641	2.640	7	47	630	1.606	1.606	9
12	002	2.578	2.579	58	48	133	1.594	1.594	9
13	400	2.565	2.565	59	49	281	1.580	1.580	12
14	241,410	2.525,2.523	2.523	49	50	172	1.564	1.564	7
15	250	2.462	2.463	17	51	631	1.533	1.533	15
16	331	2.434	2.435	12	52	143	1.526	1.526	15
17	151	2.397	2.397	13	53	532	1.519	1.519	5
18	122	2.355	2.356	1	54	471	1.510	1.510	8
19	411	2.267	2.267	2	55	323	1.500	1.500	5
20	430	2.249	2.249	3	56	243	1.478	1.478	18
21	251	2.222	2.222	18	57	641	1.473	1.473	12
22	341	2.212	2.212	8	58	542	1.460	1.460	18
23	132	2.205	2.205	5	59	082	1.450	1.450	26
24	222,421	2.189,2.183	2.186	6	60	462,182	1.436	*	5
25	061	2.130	2.129	6	61	651	1.405	1.405	18
26	161	2.085	2.087	6	62	423,730	1.399	*	5
27	042	2.077	2.077	11	63	063	1.385	*	6
28	232	2.067	2.068	14	64	721,571	1.382,1.381	*	6
29	431	2.062	2.061	6	65	163	1.373	*	4
30	142	2.036	2.036	5	66	632	1.363	1.363	10
31	351	2.000	2.000	8	67	2,10,0	1.353	1.353	17
32	322	1.976	1.976	5	68	353	1.347	1.347	15
33	511	1.890	1.890	2	69	482	1.262	1.262	14
34	270	1.867	1.867	3	70	643	1.146	1.146	18
35	171	1.838	*	1	71	2,12,1	1.113	1.113	31
36	402	1.819	1.818	10					

Note. Asterisked d_{obs} indicates weak line not used in unit cell refinement.

$\frac{1}{4}(0,2,0)^*$, and $\mathbf{c}^* = \frac{1}{2}(\bar{2},0,2)^*$. Note also the doubled density of reflections along the $\mathbf{b}^*$ direction in the First Order Laue Zone (FOLZ) of the [100] zone axis CBP. The extinction condition obeyed by the Zero OLZ (ZOLZ) reflections at this zone axis—namely $F(0kl)^* = 0$ unless $k = 2n$—requires the structure to have a *b* glide perpendicular to **a**. This is confirmed by Fig. 3(b). Similarly, the extinction condition obeyed by the ZOLZ reflections at the [001] zone axis—namely $F(hk0)^* = 0$ unless $h = 2n$—requires an *a* glide perpendicular to **c**. The space group of low-carnegieite is therefore Pb_a, in agreement with the conditions observed by XRD. There are only two possible space groups compatible with these requirements—namely $Pb2_1a$ or *Pbma*. They

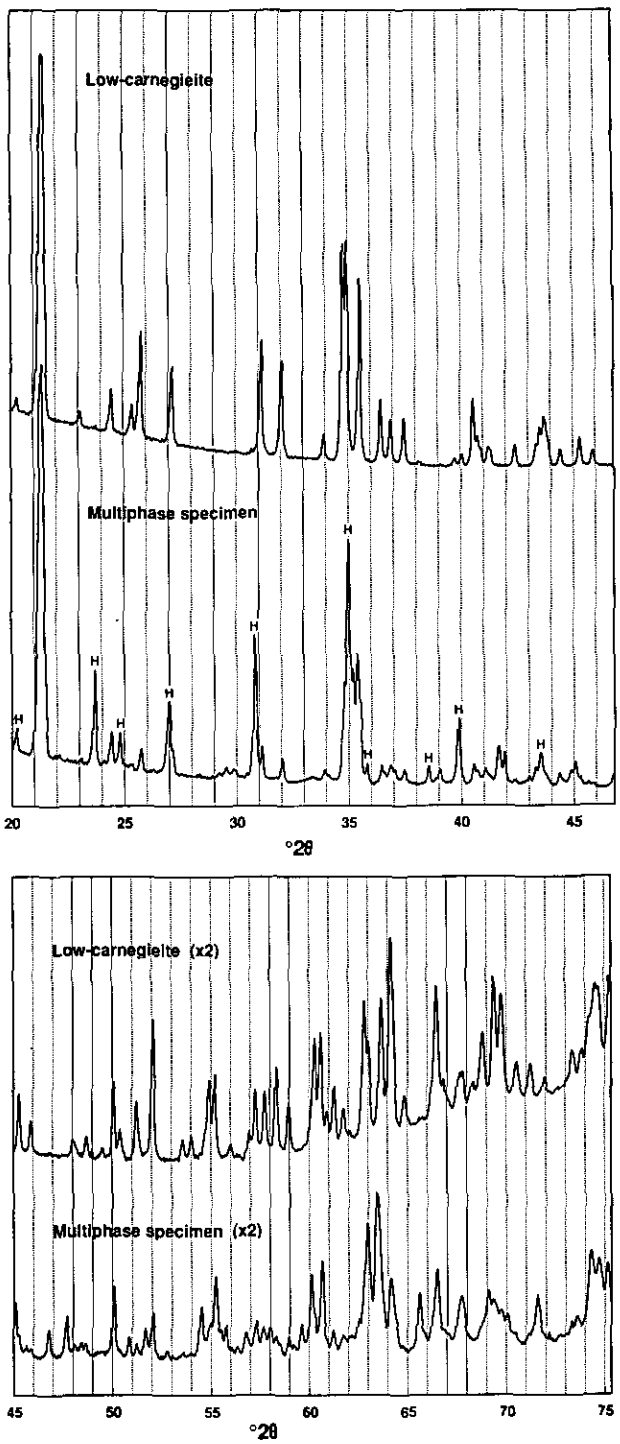

FIG. 2. Densitometer traces from the Guinier–Hägg films for both low-carnegieite and a 1 : 1 : 1 multiphase specimen (λ = 1.5406Å). In the lower trace lines corresponding to the hexagonal phase are marked by **H**.

TABLE II

COMPARISON OF POWDER DIFFRACTION DATA WITH PREVIOUS WORK

Multiphase specimen			Klingenberg and Felsche (1981)	
d_{obs}	I/I_0	Assignment	d_{obs}	I/I_0
4.390	6	Hex 211 + C	4.394	11
4.180	100	C	4.182	83
4.153	100	C	4.165	100
3.849	1	C		
3.757	23	Hex 004	3.759	25
3.640	8	C	3.644	8
3.589	8	Hex 104	3.588	11
3.462	6	C		
3.306	18	Hex 114	3.310	17
			3.302	24
3.285	6	C		
3.020	2	Hex 400		
2.991	2	unidentified		
2.902	37	Hex 214	2.900	51
2.872	8	C		
2.794	6	C	2.794	3
2.641	3	C		
2.579	24	C		
2.561	61	Hex 224	2.562	95
2.550	30	C	2.551	47
2.536	33	C?	2.538	49
2.524	22	C	2.528	17
2.505	5	Hex 006	2.507	6
2.464	4	C	2.456	3
2.439	4	C	2.443	5
2.401	3	C		
2.332	4	Hex 330	2.335	8
			2.315	1
2.305	3	Hex 502	2.305	7
2.257	17	Hex 121	2.260	29
2.224	5	C		
2.214	4	C	2.215	5
2.197	4	Hex 216	2.197	5
			2.167	13
2.164	10	Hex 414	2.165	13
2.152	8	Hex 511	2.154	10
			2.102	4
2.090	4	Hex 512 + C	2.088	6
			2.080	7
2.078	8	Hex 423	2.076	10
2.036	4	Hex 226	2.042	4
			2.018	5
2.007	6	Hex 316	2.009	9

C = low-carnegieite, Hex = hexagonal phase.

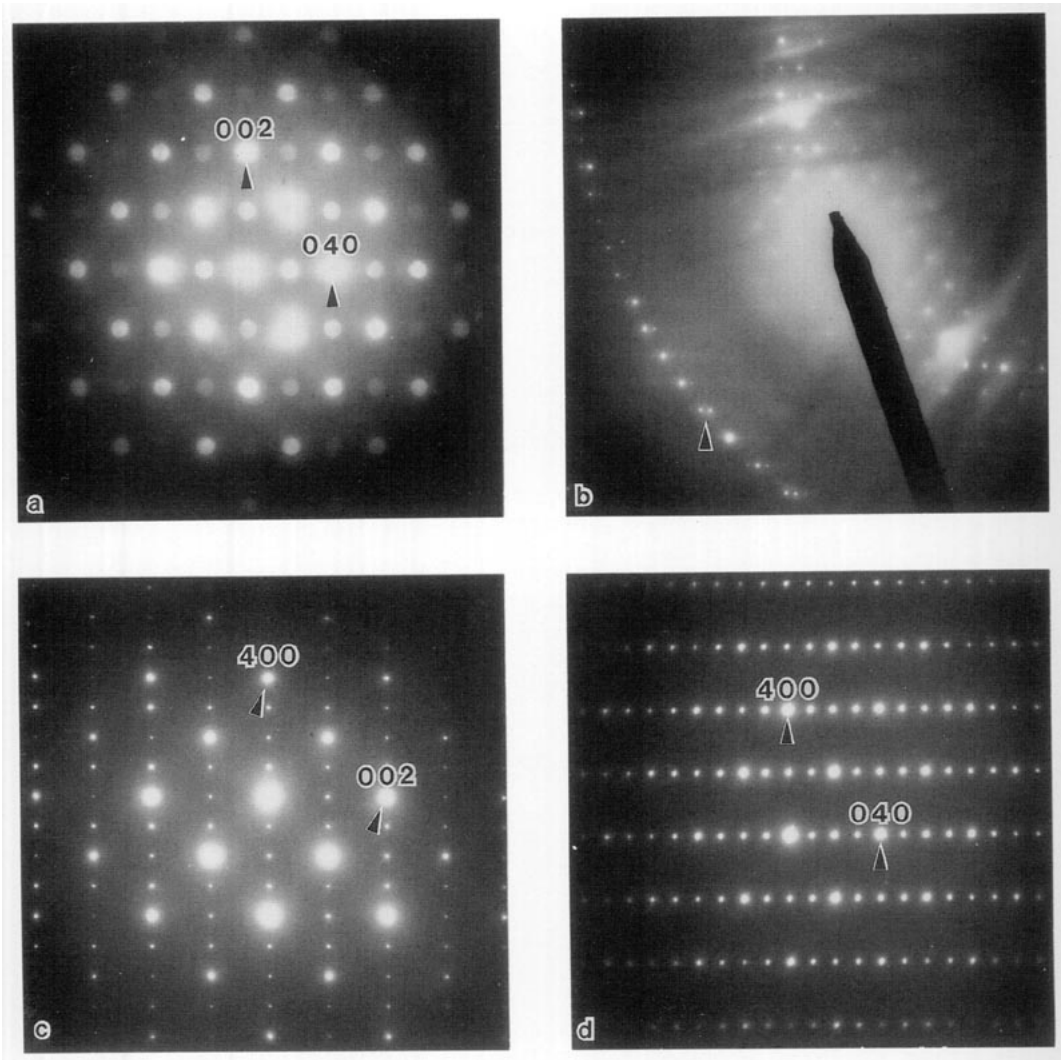

FIG. 3. Shows (a) a [100] zone axis Convergent Beam Pattern (CBP), (b) a corresponding Selected Area Diffraction Pattern (SADP) but taken tilted a few degrees off [100], (c) an [010] zone axis SADP, and (d) an [001] zone axis SADP of single phase low carnegieite. The indexing is with respect to the low-carnegieite cell given in the text.

differ only in that the latter contains an inversion center whereas the former does not. Given that the NMR and electron microprobe results (both discussed below) unequivocally confirm that the Al and Si atoms are perfectly ordered in low-carnegieite, i.e., each AlO_4 tetrahedron is tetrahedrally coordinated by four SiO_4 tetrahedra and vice versa, it follows that it is not possible for the structure to possess an inversion centre and hence the only possible space group is $Pb2_1a$.

TEM examination of the earlier multiphase material showed several different types of well-crystallized, high-carnegieite-related phases. Diffraction patterns were

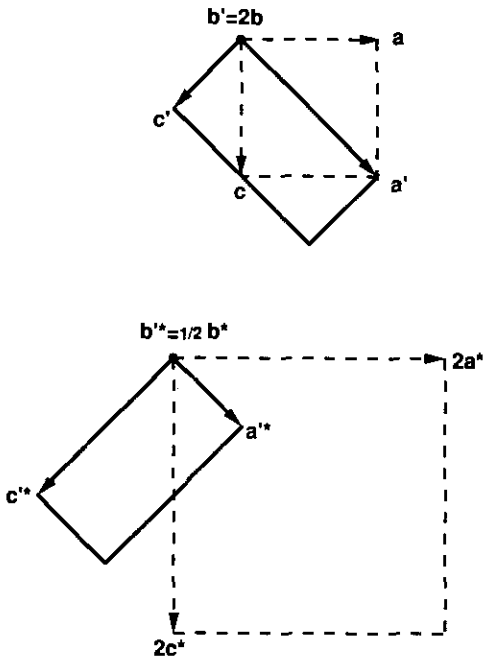

FIG. 4. Shows the real and reciprocal space unit cell relationships between the $F\bar{4}3m$, high-carnegieite-type, average structure (unprimed) and the $Pb2_1a$ low-carnegieite structure (primed).

obtained (see Fig. 5) in which the strong reflections were always clearly related to an underlying $F\bar{4}3m$, high-carnegieite-type, average structure—a variety of weaker satellite reflections, however, could be observed. These extra satellite reflections were generally characterized by modulation wave-vectors of either $\frac{1}{4}$ or $\frac{1}{3}\{1,1,1\}^*$ type, $\frac{1}{3}\{0,2,0\}^*$ type or $\frac{1}{4}\{0,2,0\}^*$ type (see Fig. 5). SADPs were often obtained which were probably due to coherent intergrowth of differently modulated types of well-crystallized, high-carnegieite-related phases (see, for example, Fig. 5(c)).

Microstructures and Compositions

The single crystalline phase low-carnegieite specimen was examined using transmitted polarized light microscopy of material that had been powdered for TEM studies. Some 50–70% of fragments were birefringent with complex twin and fracture structures. The remaining 30–50% was optically isotropic and, from its cleavage shapes, was inferred to be glass. This agreed with the common occurrence of amorphous fragments in electron diffraction studies.

A polished section was prepared from one solid piece (~10 mm^3) of the preparation for examination by electron microprobe. Using backscattered electrons, two phases could be detected in the material (Fig. 6). The phase with higher $\bar{Z}$ was continuous and, from a region at the edge of the polished specimen where this phase was concentrated, it could be correlated with the glassy material noted above. The other phase, lower in average atomic number $\bar{Z}$, was discrete and highly fractured and, by default, the crystalline phase. Given that the carnegieite structure undergoes significant distortion with a corresponding reduction in unit cell volume when it transforms from the high- to the low-temperature structure the observed microstructure confirms this to be low-carnegieite.

Six electron microprobe analyses were made on regions of each of the two phases with the following results (Analyses of the glass were made with beam scanning across an area of 150 μm^2 to minimize volatilization, but analytical totals were still low by an average of 2.4%):

Crystalline phase:

$$Na_{1.012(5)}\ Al_{0.999(3)}\ Si_{0.997(3)}\ O_4.$$

Glass phase:

$$Na_{0.67(5)}\ Al_{1.005(6)}\ Si_{0.995(6)}\ O_{3.83}\ (\text{plus } Fe_{0.003}).$$

Oxygen in these analyses is assumed from oxide stoichiometry and the results are reported with (i) total oxygen normalized to 4 atoms for the crystalline phase and (ii) Al + Si normalized to 2 for the glass phase. The glass phase is clearly variable in composition with a range of recalculated Na content between 0.63 and 0.78. These compositions are consistent with the observed $\bar{Z}$

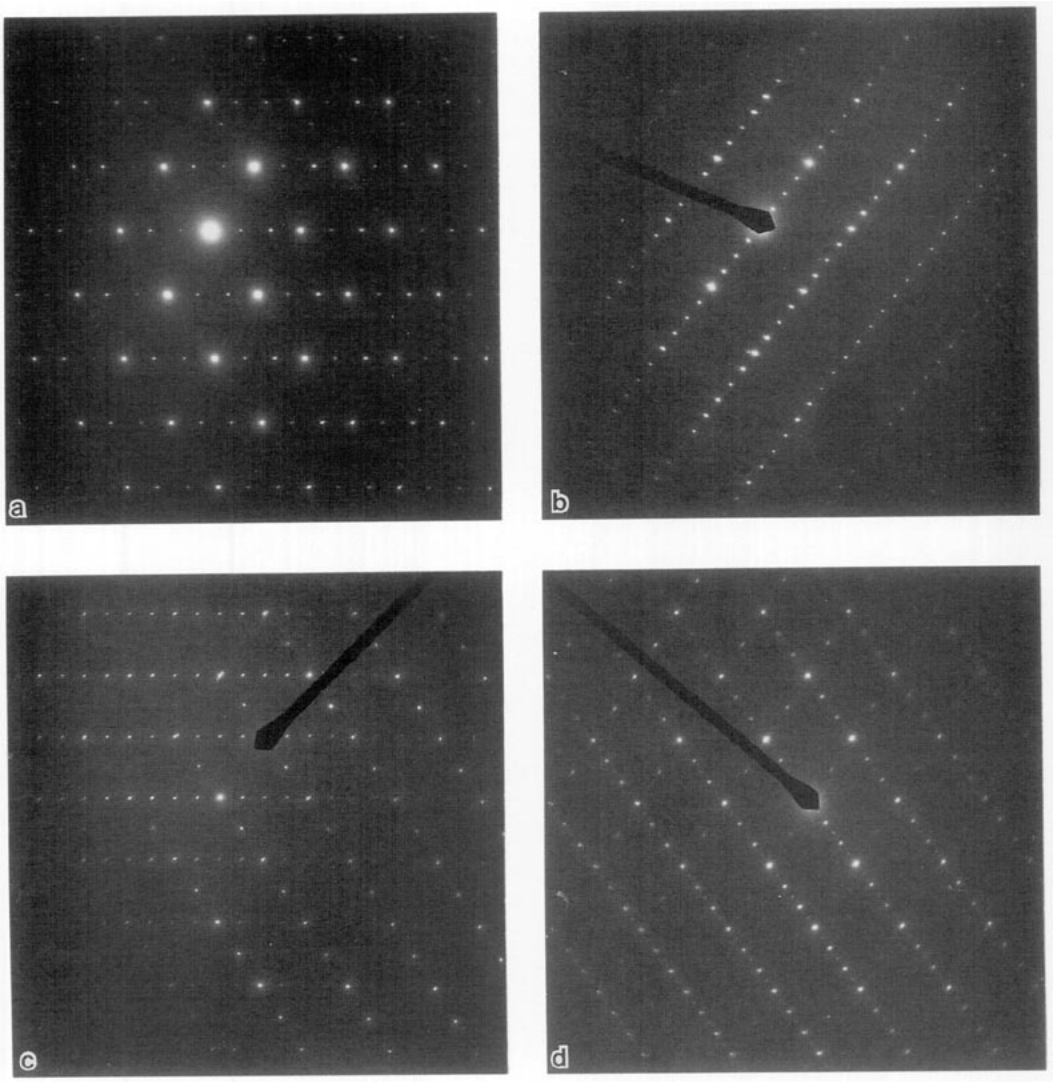

FIG. 5. Typical high-carnegieite-related ⟨110⟩ (with respect to the underlying, $F\bar{4}3m$, high-carnegieite-type parent structure) zone axis SADPs obtained from the earlier half-baked, multi-phase material. The first strong (parent) reflection in the horizontal direction is of {002}* type while the first parent reflection in the vertical direction is of {220}* type. Thus satellite reflections of $\frac{1}{4}\{0,2,0\}^*$ type are present in (a), of $\frac{1}{4}\{1,1,1\}^*$ type in (b), of $\frac{1}{4}\{0,2,0\}^*$ type in (c), and of $\frac{1}{4}\{1,1,1\}^*$ type in (d).

contrast from backscattered electron images: ideal $NaAlSiO_4$ has $\overline{Z}$ = 10.62, whereas the average glass composition effectively is deficient in Na_2O ($\overline{Z}$ for Na_2O = 10.23) and therefore has a higher $\overline{Z}$ calculated at 10.66.

^{29}Si and ^{27}Al NMR spectra

^{29}Si MAS NMR spectra are presented in Fig. 7 for both the low-carnegieite and the 1 : 1 : 1 multiphase specimen described above under XRD. The spectrum for low-

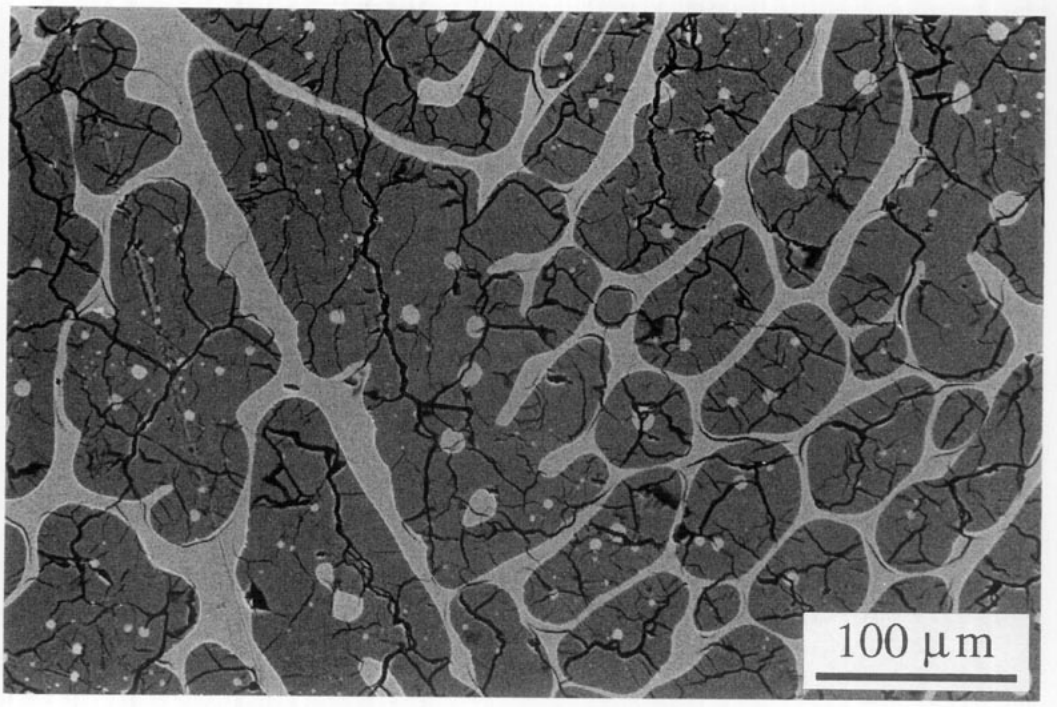

FIG. 6. Microstructure of the single crystalline phase low-carnegieite specimen corresponding to the XRD profile in Fig. 2. In this backscattered electron image, intensity is proportional to the average atomic number $\overline{Z}$. The darker, lower $\overline{Z}$ regions are carnegieite while the lighter, higher $\overline{Z}$ regions represent a continuous glass phase. Note that fractures (thin black lines in the image) are confined almost exclusively to regions of crystal.

carnegieite shows a single sharp signal (FWHM = 105 Hz) at −81.8 ppm. This is superimposed on a broad hump centered on ~ −88 ppm. Given the large proportion of glassy material observed by both optical and electron microscopy as well as in the microprobe we conclude that the broad hump corresponds to the glassy phase and the single, sharp signal to the low-carnegiite.

By reference to previous ^{29}Si NMR studies of framework aluminosilicates, and zeolites in particular, we can conclude that the sharp signal at −81.8 ppm corresponds to a Si(4Al) environment. The Na-containing zeolites, sodalite and thomsonite, which also have Si in a Si(4Al) environment, give −84.8 and −83.5 ppm, respectively (*12*). While it is true that this result does not preclude a Si : Al ratio of <1.0 it does rule out that Si : Al > 1.0. Together with the electron microprobe analysis we can conclude that low-carnegieite has the stoichiometry $NaAlSiO_4$ and that there is perfect Si : Al ordering; i.e., each Si is surrounded by 4 Als and vice versa.

By comparison, the ^{29}Si MAS NMR spectrum of the 1 : 1 : 1 multiphase specimen gave a much broader signal (FWHM = 185 Hz, δ = −82.3 ppm) than that for low-carnegieite. For this material there is no broad signal corresponding to a glassy phase and this is born out by observations in the optical microscope. It is known that substitution of Al for nearest neighbor Si in an isostructural series increases the chemical shift by 5–6 ppm (*12*, *13*). Therefore we

can infer from the absence of any significant signal with lower chemical shift that Si in all the phases present, i.e., low-carnegieite, the hexagonal phase, and other unidentified phases, occurs in a Si(4Al) environment.

The ^{27}Al MAS NMR spectra for the same two specimens are presented in Fig. 8. Tetrahedrally coordinated Al is known to fall in the region 50 to 80 ppm. Both spectra give signals corresponding to Al in a tetrahedral environment. The ^{27}Al signal for low-carnegieite is quite sharp (FWHM = 300 Hz, δ = 58.9 ppm) and symmetric, indicating that the Al present in the low-carnegiite and the glassy phase is in a highly symmetric tetrahedral environment. On the other hand the signal for the multiphase specimen (FWHM = 500 Hz, δ = 57.4 ppm) is somewhat broader and moderately asymmetric. This asymmetry is not necessarily due to some Al being present in higher oxygen coordination. It is more probably a result of lower symmetry of the tetrahedral AlO_4 environment giving rise to second order quadrupolar broadening effects which are not removed by magic-angle spinning (MAS) (*14, 15*). It is evident from both the ^{27}Al NMR spectra that there is no octahedral Al present in either specimen. For the 1 : 1 : 1 multiphase specimen this is consistent with the absence of β- or β''-alumina diffraction lines.

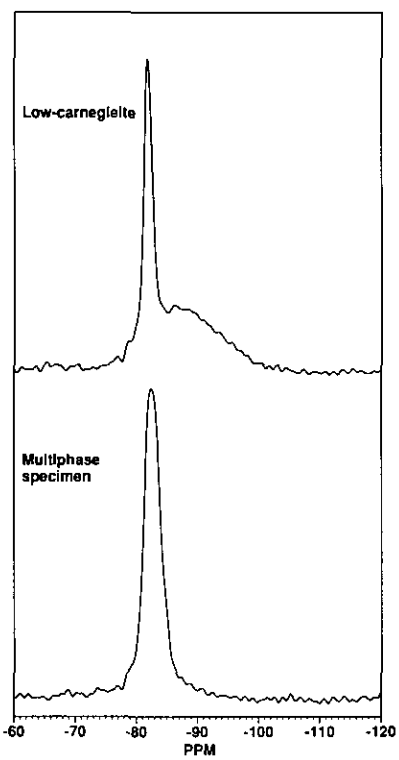

FIG. 7. ^{29}Si MAS NMR spectra of low-carnegieite (upper) and a 1 : 1 : 1 multiphase specimen (lower). Chemical shifts are relative to TMS.

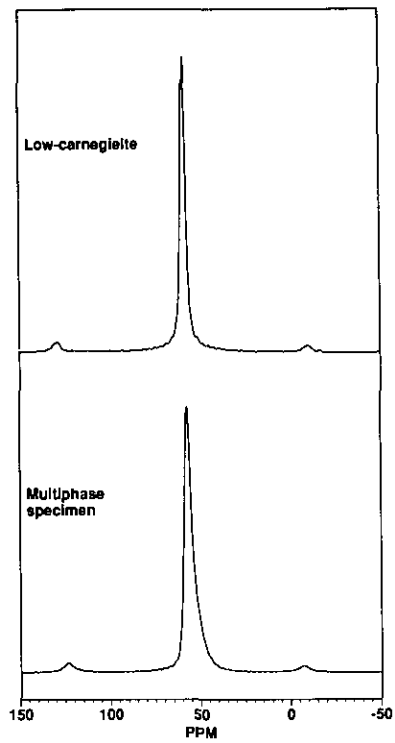

FIG. 8. ^{27}Al MAS NMR spectra of low-carnegieite (upper) and a 1 : 1 : 1 multiphase specimen (lower). Chemical shifts are relative to $Al(H_2O)_6^{3+}$.

Discussion

Comparison with Previous Work

The materials previously described (*7–9*) as being low-carnegieite were almost cer-

tainly multiphase mixtures. This has only become evident following the successful synthesis of the single crystalline phase material described in this work and by careful analysis using a range of techniques of the materials prepared under the conditions described by Klingenberg and Felsche (*7*).

The TEM and XRD analyses of our multiphase specimens confirmed that there was some low-carnegieite present in the phase mixtures, but that a large proportion of these specimens was not low-carnegieite. EDS analysis of these other phases indicated that their stoichiometry was, in general, close to that of $NaAlSiO_4$. However, the extraordinary variability in their electron diffraction patterns and the inability to correlate their electron diffraction patterns with the XRD data meant that it was not possible to further characterize these other phases.

Attempts to prepare the hexagonal phase, described above, as a single phase were unsuccessful, and neither was it possible to observe electron diffraction patterns corresponding to its proposed unit cell. Nevertheless, the lines corresponding to this phase were present in all the earlier reported XRD data for "low-carnegieite."

Close relationship to $Na_4Mg_2Si_3O_{10}$

The space group and unit cell of low-carnegieite having been determined ($Pb2_1a$, $a = 10.261(1)$, $b = 14.030(2)$, $c = 5.1566(6)$ Å) it was of particular interest to discover the space group and unit cell reported for $Na_4Mg_2Si_3O_{10}$. An initial investigation of this material (*16*) reported a unit cell very similar to low-carnegieite but with a halved b axis. Subsequently, Foris *et al.* (*17*) determined the unit cell for this compound using a combination of precession photography of severely twinned single crystals and XRD using a Guinier–Hägg camera as P_a, $a = 10.584(7)$, $b = 14.328(7)$, $c = 10.457(7)$ Å. Apart from small differences in the unit cell dimensions and a doubled c axis, the two compounds appear to be almost isostructural. A cursory comparison of the relative intensities of equivalent XRD lines between Table 1 of Foris *et al.* (*17*) and Table I of the present work confirms this view.

If we apply the same description to $Na_4Mg_2Si_3O_{10}$ that we have presented for carnegieite, namely a "stuffed" derivative of cristobalite in which some of the cavities in the SiO_2 framework are filled with sodium atoms (Fig. 1), the analogy becomes clearer. In $Na_4Mg_2Si_3O_{10}$, we now have $\frac{2}{5}$ of the Si sites occupied by Mg instead of $\frac{1}{2}$ filled by Al as in carnegieite. In addition the Na occupies $\frac{4}{5}$ of the cavities in the framework instead of $\frac{1}{2}$ as in carnegieite. Despite these differences the two compounds both distort from their high-temperature cubic structure in a remarkably similar way. Even the high $\leftrightarrow$ low phase transition temperatures are almost identical; 940 ± 5 K for $NaAlSiO_4$ (*7*), 893–918 K for $Na_4Mg_2Si_3O_{10}$ (*16*).

Difficulty in Synthesizing Low-Carnegieite

From our own experience and that of earlier workers it is reasonable to propose that the synthesis of single phase low-carnegieite is difficult. Preparing low-carnegieite by reaction of the component "oxides" results in two conflicting processes. Firstly, the complete mixing of the components is extremely sluggish, even at temperatures just below the solidus. Secondly, at temperatures that facilitate the laboratory time-scale growth of low-carnegieite from its component "oxides", Na_2O is readily lost to the atmosphere.

The electron microprobe data from the single crystalline phase material, while confirming the expected stoichiometry for the low-carnegieite, also showed the Na_2O deficiency of the glass. While the starting mixture had the correct stoichiometry for $NaAlSiO_4$, a substantial amount of Na_2O must have been lost when the mixture was annealed at 1673 K and/or when it was

melted at 1873 K for 1 hr. We surmise that, following the loss of Na_2O, the composition of the system placed it in a two-phase, solid + liquid, region of the temperature–composition phase diagram for the temperature of synthesis. However, there is insufficient detail in the literature to verify this.

Certainly the observation of multiple phases and incomplete reaction for specimens prepared at lower temperatures is consistent with the proposition that the kinetics of formation of fully ordered, single-phase low-carnegieite are sluggish.

Conclusions

The incorrect indexing of XRD data in previous studies, and in particular by Klingenberg and Felsche (*7*), illustrates the need to proceed cautiously when confronted by a complicated unknown powder diffraction pattern. While it may be possible to completely index all the lines to a particular unit cell, this achievement is not a sufficient condition for that unit cell to be correct, nor for only one crystalline phase to be present. Heeding our own caution we acknowledge that the large hexagonal unit cell proposed for the new phase identified in this study may not be the correct one.

The main advantage that the present study had over previous work was the understanding of low-carnegieite as a modulated form of high-carnegieite. First, this allowed us to identify the problem with the very strong superstructure lines proposed by Klingenberg and Felsche (*7*). Second, the electron diffraction patterns could be correctly indexed in terms of the dominant parent reciprocal lattice. The complementary nature of the various spectroscopic and diffraction techniques used in this study ensured that if a unique explanation could be found for all the experimental results it would necessarily be convincing.

The space group, unit cell, composition, and Si : Al ordering of low-carnegieite having been resolved, there still remains the question of its crystal structure. While the connectivity of the tetrahedral aluminosilicate framework is determined, both the angular distortions of that framework with respect to the ideal high-cristobalite-like framework and the ordering of the Na atoms over the two cavity sites are as yet unresolved. Further work is in progress toward this goal.

Acknowledgments

The authors thank Dr N. G. Ware for carrying out the electron probe analyses and for instructions on the physics of $\overline{Z}$ contrast imaging. Messrs. K. Owen and N. Gabbitas are also acknowledged for helping in the preparation of the XRD and NMR figures, respectively.

References

1. M. J. Buerger, *Z. Kristallogr. A* **90,** 186–192 (1935).
2. M. O'Keeffe and B. G. Hyde, *Acta Crystallogr. Sect. B* **32,** 2923–2936 (1976).
3. J. F. Schairer, and N. L. Bowen, *Am. J. Sci.* **254,** 129–195 (1956).
4. R. N. Abbott, *Am. Mineral.* **69,** 449–457 (1984).
5. T. F. W. Barth and E. Posnjak, *Z. Kristallogr.* **81,** 135–141 (1932).
6. C. Hermann, O. Lohrmann, and H. Philipp (Eds.), "Strukturberichte," Vol. II, pp. 158–159 (1928–1932).
7. R. Klingenberg and J. Felsche, *J. Appl. Crystallogr.* **14,** 66–68 (1981).
8. J. V. Smith and O. F. Tuttle, *Am. J. Sci.* **255,** 282–305 (1957).
9. R. D. Shannon and I. Berzins, *Mater. Res. Bull.* **14,** 361–367 (1979).
10. W. Borchert and J. Keidel, *Heidelberg. Beitr. Mineral. Petrog.* **1,** 2–16 (1947).
11. R. Klingenberg and J. Felsche, *J. Solid State Chem.* **61,** 40–46 (1986).
12. E. Lippmaa, M. Mägi, A. Samoson, M. Tarmak, and G. Engelhardt, *J. Am. Chem. Soc.* **103,** 4992–4996 (1981).

13. J. M. NEWSAM, *J. Phys. Chem.* **89,** 2002–2005 (1985).

14. R. J. KIRKPATRICK, "Reviews in Mineralogy, Vol. 18, Spectroscopic Methods in Mineralogy and Geology" (F. C. Hawthorne, Ed.), pp. 341–403, Mineralogical Society of America, Washington, DC (1988).

15. S. C. KOHN, R. DUPREE, AND M. E. SMITH, *Geochim. Cosmochim. Acta* **53,** 2925–2935 (1989).

16. R. D. SHANNON, *Phys. Chem. Miner.* **4,** 139–148 (1979).

17. C. M. FORIS, F. C. ZUMSTEG, AND R. D. SHANNON, *J. Appl. Crystallogr.* **12,** 405–406 (1979).